Hydride CVD Hetero-epitaxy of $B_{12}P_2$ on 4H-SiC

C.D. Frye[a,b], C.K. Saw[a], Balabalaji Padavala[b], R.J. Nikolić[a], J.H. Edgar[b]

[a]*Lawrence Livermore National Laboratory, Livermore, CA 94550*
[b]*Kansas State University, Department of Chemical Engineering, Durland Hall, Manhattan, KS 66506*

Abstract

Icosahedral boron phosphide ($B_{12}P_2$) is a wide bandgap semiconductor (3.35 eV) that has been reported to "self-heal" from high-energy electron bombardment, making it attractive for potential use in radioisotope batteries, radiation detection, or in electronics in high radiation environments. This study focused on improving $B_{12}P_2$ hetero-epitaxial films by growing on 4H-SiC substrates over the temperature range of 1250-1450 °C using B_2H_6 and PH_3 precursors in a H_2 carrier gas. XRD scans and Laue transmission photographs revealed that the epitaxial relationship was $(0001)\langle 11\bar{2}0\rangle_{B_{12}P_2} \| (0001)\langle 11\bar{2}0\rangle_{4H\text{-}SiC}$. The film morphology and crystallinity were investigated as a function of growth temperature and growth time. At 1250 °C, films tended to form rough, polycrystalline layers, but at 1300 and 1350 °C, films were continuous and comparatively smooth ($R_{RMS} \leq 7$ nm). At 1400 or 1450 °C, the films grew in islands that coalesced as the films became thicker. Using XRD rocking curves to evaluate the crystal quality, 1300 °C was the optimum growth temperature tested. At 1300 °C, the rocking curve FWHM decreased with increasing film thickness from 1494 arcsec for a 1.1 μm thick film to 954 arcsec for a 2.7 μm thick film, suggesting a reduction in defects with thickness.

Keywords:
A3. Chemical vapor deposition processes, A3. Hydride vapor phase epitaxy, B1. Borides, B2. Semiconducting boride compounds

1. Introduction

Two boron phosphide compound semiconductors exist: cubic, zincblende BP and rhombohedral $B_{12}P_2$, which is often referred to as boron subphosphide or icosahedral boron phosphide. Icosahedral boron phosphide derives its name from the B_{12} icosahedra centered on each vertex of its rhombohedral unit cell and features interlinking phosphorus-phosphorus chains along the body diagonal in the [111] direction ([0001] direction of the hexagonal unit cell). Note: hexagonal indices will be used throughout this report unless otherwise noted to maintain consistent indices between the epitaxial film and substrate.

$B_{12}P_2$ has garnered interest due to its wide bandgap of 3.35 eV[1], chemical inertness, and reported ability to withstand intense bombardment from high-energy electrons without agglomerating defects or becoming amorphous[2, 3, 4]. These properties make $B_{12}P_2$ attractive as a material in radiation detection, electronics located in high radiation environments, or in radioisotope batteries. Unfortunately, $B_{12}P_2$ crystal growth is still in its early stages, and poor material quality has limited the detailed characterization of radiation induced effects on its electronic properties and prevented the fabrication of $B_{12}P_2$ diodes. Thus, improving crystal growth is essential to evaluating its potential as an electronic material.

Native $B_{12}P_2$ substrates are not commercially available, thus a variety of non-native substrates have been previously employed for the growth of $B_{12}P_2$ thin films, including Si[5, 6, 7, 8, 9, 10], sapphire[5], MgO[5], SiO_2[5, 8], Ni[8], W[8], and most recently 6H-SiC[11]. Although silicon has been the most common substrate for VPE-grown $B_{12}P_2$ reported in the literature, the symmetry mismatch of the (100) and (110) faces, the large lattice constant mismatch (22.0%) for the (111) face, and thermal instability of silicon at high growth temperatures (melting point = 1414 °C) make it a poor substrate for the epitaxial growth of $B_{12}P_2$.

Several promising crystalline substrates have become available in the years since the majority of the reports of $B_{12}P_2$ epitaxial growth were published. For instance, GaN and AlN bulk substrates and template films on sapphire

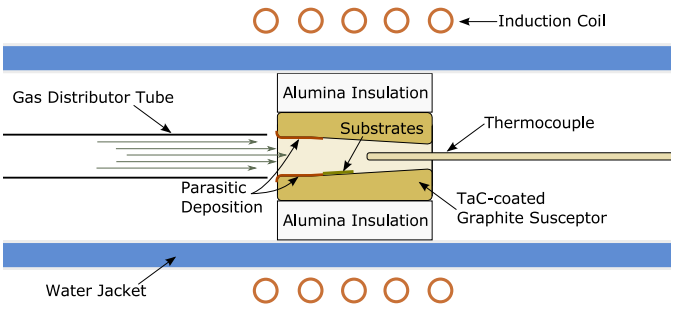

Figure 1: A schematic of the CVD reactor used in this study.

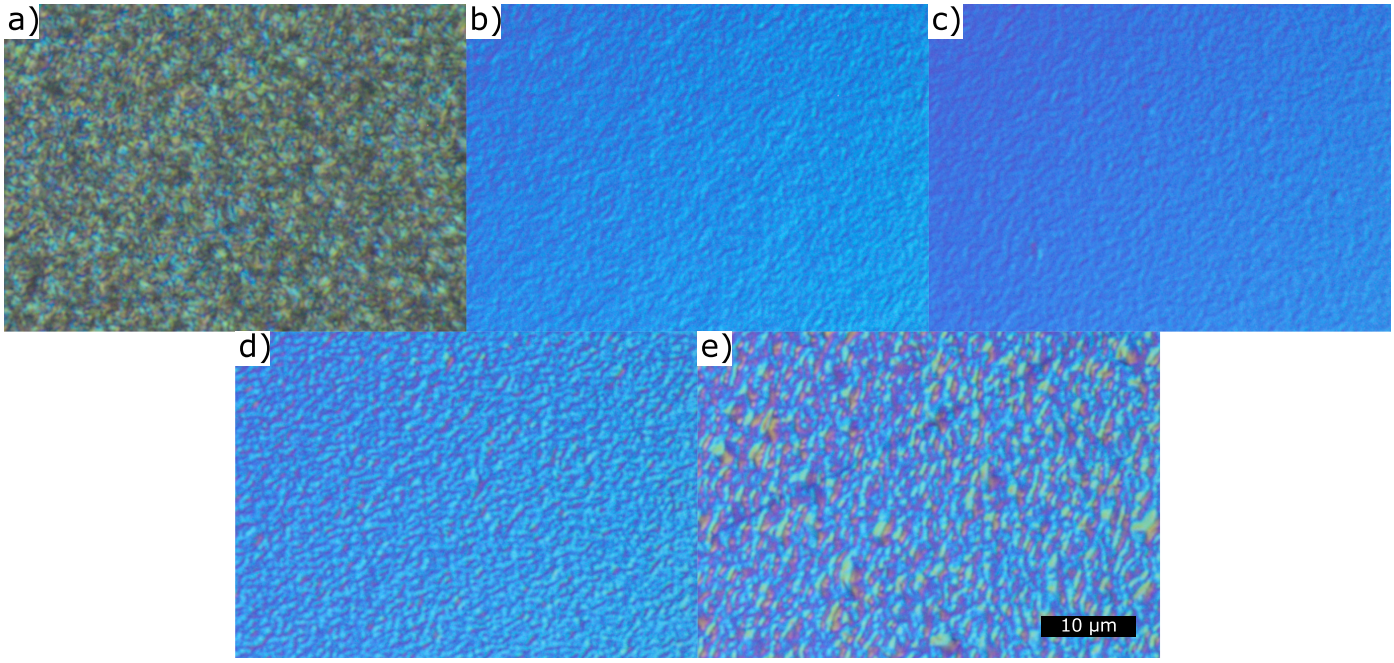

Figure 2: Nomarski interference optical micrographs of $B_{12}P_2$ films grown on 4H-SiC tilted 4° towards the $(1\bar{1}00)$ at a) 1250 °C, b) 1300 °C, c) 1350 °C, d) 1400 °C, and e) 1450 °C. The scale bar is the same for all images and is 10 μm. At 1250 °C, the film is rough and polycrystalline. The films become smooth when the growth temperature is increased to 1300-1350 °C but become rougher as the temperature is further increased. R_{RMS} roughness measurements for these films can be found in TABLE 1.

are now commercially available. SiC is also now widely available. Although there have been several reports of BP growth on SiC[12, 13, 14, 15], Lu, *et al.*[11] have provided the only report of $B_{12}P_2$ growth on SiC where BBr_3 and PBr_3 in H_2 was used to deposit $B_{12}P_2$ on 6H-SiC. However, the maturity, quality and availability of bulk SiC substrates has greatly improved in the ten years since Lu *et al.*'s study.

SiC is an appealing substrate for numerous reasons. First, unlike Si, SiC has a hexagonal lattice which is compatible with the rhombohedral unit cell of $B_{12}P_2$, which can also be represented as a hexagonal system. Furthermore, the 3.073 Å a-lattice constant of SiC is approximately half that of the $B_{12}P_2$ a-lattice constant of 5.99 Å[16], giving an effective lattice mismatch of ∼2.5%. SiC is also inert and thermally stable above the melting point of Si, extending the growth window in which $B_{12}P_2$ can be deposited. Additionally, an n-type SiC/p-type $B_{12}P_2$ heterojunction diode could be fabricated using an n-type SiC substrate, similar to the work of Gong, *et al.*[17] for $B_{12}As_2$ on SiC. Moreover, carefully choosing the miscut direction of 4H-SiC can reduce the density of twin domains in hetero-epitaxially grown films[12, 18, 19].

Here, $B_{12}P_2$ is grown over the temperature range of 1250-1450 °C on 4H-SiC miscut 4° to the $(1\bar{1}00)$ to coarsely optimize the growth temperature. This study is only the second report of $B_{12}P_2$ growth on SiC and is the first using hydride precursors and SiC substrates. Further, it is the first study to report $B_{12}P_2$ XRD rocking curve data. By optimizing the growth temperature, this study lays the ground work for improved $B_{12}P_2$ films that will enable the evaluation of the electrical properties of $B_{12}P_2$ in conjunction with its radiation hardness.

2. Experimental Methods

$B_{12}P_2$ films were grown on 4H-SiC substrates in a home-built, horizontal, cold-walled CVD system (Figure 1). Details on the setup can be found elsewhere[20]. The precursors were B_2H_6 and PH_3 diluted in a H_2 carrier gas purified by a palladium membrane purifier. The 4H-SiC substrates were 10×10 mm^2 squares and were 350 μm thick. Two substrates were placed inside a tubular TaC-coated graphite susceptor, which was enclosed in alumina insulation, and heated inductively via a RF coil. The precursor and carrier gases passed through a quartz distributor tube and over the heated substrates. The temperature was measured with an alumina-sheathed thermocouple centered in the susceptor downstream of the substrates. The thermocouple was calibrated by melting a 300-500 μm thick piece of Si in the same position as a substrate in the susceptor.

Prior to loading into the reactor, the substrates were sequentially sonicated in tetrachloroethylene, isopropyl alcohol, and methanol for 5 min each to remove particulates and any organic residue. Once the substrates and the susceptor were loaded, the reactor was evacuated to <75 mTorr and backfilled with H_2 three times to remove air from the system before maintaining the carrier gas flow rate at 3.5 slm of H_2 at 100 Torr. The substrates were heated to 1650 °C for 20 min to etch the surface in prepa-

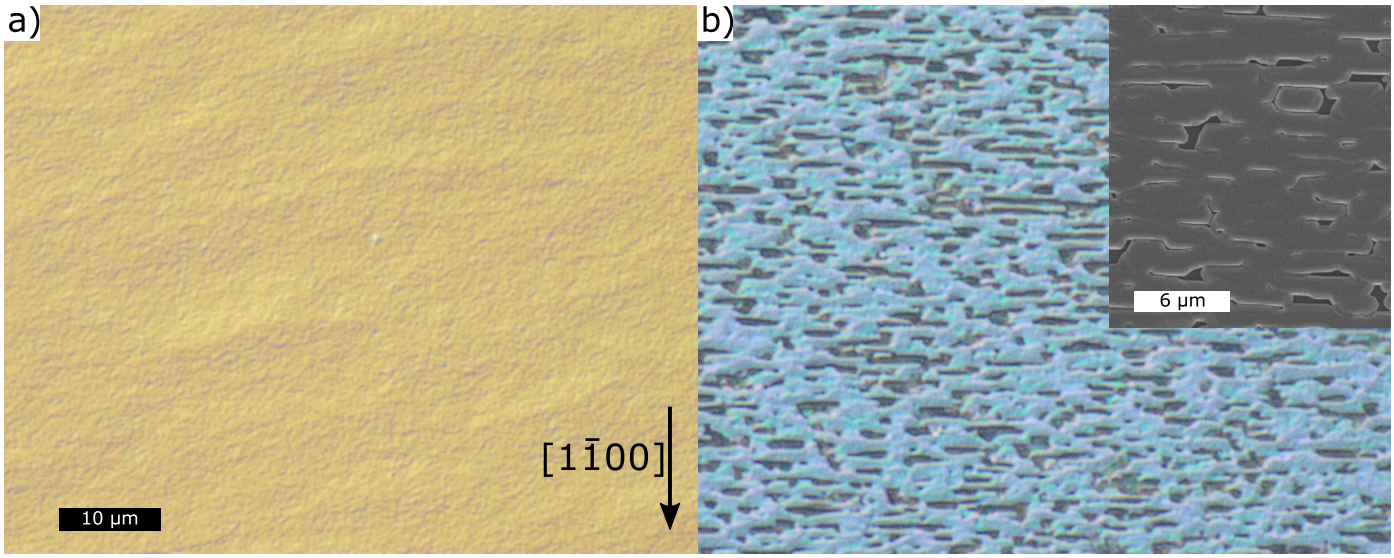

Figure 3: Nomarski interference micrographs of $B_{12}P_2$ films grown at a) 1300 °C and b) 1400 °C for 15 min (black scale bar = 10 μm and is the same for both optical images). Inset shows an SEM micrograph of the $B_{12}P_2$ film in b) (white scale bar = 6 μm). At 1400 °C, the $B_{12}P_2$ film grows in elongated islands while growth at 1300 °C is continuous.

ration for epitaxy, which removes any impurities or surface oxide[21, 22]. Then, the substrates were cooled to the growth temperature. Next, a PH_3 flow rate of 6 sccm was introduced into the reactor and flowed over the substrates for 2 min. The deposition was initiated by introducing 80 sccm of 1% B_2H_6 in H_2. The reaction was terminated by switching off the B_2H_6 flow and allowing PH_3 to flow for 2 min as any remaining B_2H_6 was reacted or flushed out of the system, turning off the PH_3 flow and waiting for 2 more min to flush out the PH_3, and then cooling the substrates from the growth temperature under H_2 flow. It was assumed that $B_{12}P_2$ did not desorb P during cooling.

$B_{12}P_2$ was grown on 4H-SiC substrates miscut 4° toward the (1$\bar{1}$00) plane over the temperature range of 1250-1450 °C in increments of 50 °C to coarsely optimize the growth temperature under these flow rates and this operating pressure. This particular miscut of 4H-SiC was chosen because it suppressed rotational twinning in films of the similar icosahedral $B_{12}As_2$[18, 19] and cubic BP[12].

The surface and growth morphology were imaged by both Normarski interference optical microscopy and scanning electron microscopy (SEM). The roughness was measured with an optical profilometer using phase-shift interferometry. To measure the film growth rates, films were diced in half in the direction of the gas flow during growth, and the cross-section was measured by SEM. The reported growth rates were determined by measuring the film thickness 5 mm downstream of the leading edge of the substrate. X-ray diffraction scans were taken to determine the out-of-plane epitaxial relationship, while Laue photographs were used to determine the in-plane epitaxial relationship. Rocking curves were taken about the (0003) $B_{12}P_2$ peak to evaluate the crystal quality of the films.

3. Results and Discussion

3.1. Surface Morphology

As a first-order gauge of the film quality and to evaluate the growth mode, the surface topology was analyzed using Nomarski interference contrast optical microscopy (FIGURE 2) and optical profilometry. For 30 min growths, the surface morphology of the films varied from continuous and smooth to rough (FIGURE 2); the surface roughness was minimized at 1350 °C (TABLE 1). At 1250 °C, the surface morphology was so rough that an accurate measurement by optical interferometry was not possible. While the 1250 °C film appeared polycrystalline in the center and on the upstream edge of the substrate, the downstream edges of the substrate exhibited a thinner film that was much smoother. The rough polycrystalline region likely started growing on top of the smoother morphology since the rough area was thicker than the smoother area and consistently decreased in area when the deposition time was reduced to 15 min from 30 min. The smooth region of the 1250 °C-grown sample strongly resembled the surface of the 1300 °C sample, which was comparatively smooth (R_{RMS} = 7 nm) and uniform over the entire substrate. However, small, isolated crystals ~3 to 5 μm in diameter were interspersed in a few areas of the 1300 °C sample. At shorter deposition times, the films have fewer of these isolated crystals, and at sufficiently short times, none form at all. At longer growth times, the concentration of the crystals increases. At 1350 °C, the film was the smoothest of any of the samples with an R_{RMS} value of 3 nm that was largely uniform over the substrate. At 1400 °C the film was rougher. At the edge of some samples, hexagonal $B_{12}P_2$ islands merged together to form a continuous film. At 1450 °C, the film was even rougher, and other crystal orientations nucleated in regions of the film. The

Table 1: R_{RMS} roughness (nm) as measured by optical interferometry, FWHM (arcsec) of the (0003) plane of $B_{12}P_2$ films grown for 30 min, and growth rate (μm/hr) of $B_{12}P_2$.

	Growth Temperature (°C)				
	1250	1300	1350	1400	1450
R_{RMS} Roughness (nm)	>100	7	3	10	19
FWHM (arcsec)	2196	1080	1224	1728	2664
Growth Rate (μm/hr)	5.3	4.2	4.3	3.1	3.5

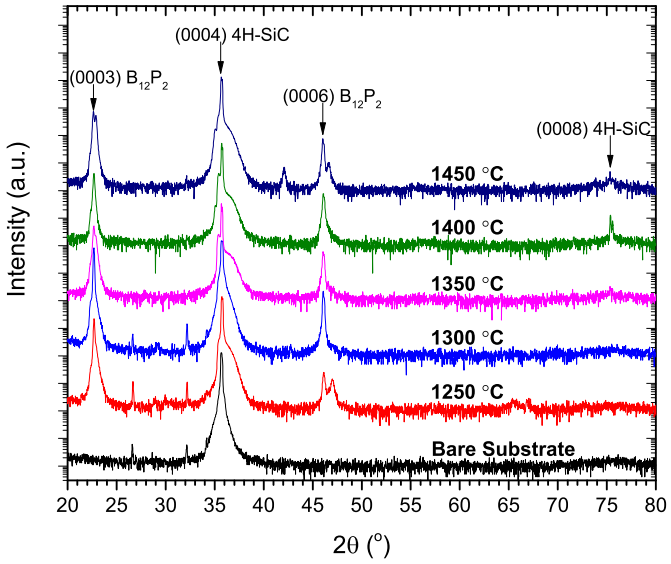

Figure 4: XRD scans of 4H-SiC substrate and $B_{12}P_2$ films grown on 4H-SiC. The y-axis is a logarithmic scale. Films grown at 1250 and 1450 °C have $(02\bar{2}4)$ doublet peaks at 46.4°, indicating that they are partially polycrystalline while the other films are single crystalline as they only have (0003) and (0006) peaks. Peaks at ≈ 26.5° and 32° originate from the 4H-SiC substrate.

non-orientated nuclei on the film may have originated from homogeneous nucleation in the gas phase above the substrate. That is, particles might form in the gas phase and land on the growing surface with a random crystal orientation. Like growth at 1400 °C, islands formed at the sample edges but were even more pronounced.

Depositions for shorter times at 1400 and 1450 °C more clearly exhibited island growth and did not form continuous films over large areas of the substrates. Typically, the islands' shapes were hexagons elongated perpendicular to the direction of miscut (see FIGURE 3 b)). The bare 4H-SiC surface after surface preparation consisted of series of stepped hillocks that were parallel to one another but perpendicular to the miscut direction. A detailed examination of the impact of the surface morphology and substrate tilt on $B_{12}P_2$ epitaxy will be reported in a future paper. The $B_{12}P_2$ films thus nucleated and grew out from the step edges of the hillocks of the substrate. In contrast, films grown at 1300 °C remained continuous for the same deposition time (FIGURE 3 a)).

3.2. Growth Rate

The growth rate of $B_{12}P_2$, measured over the temperature range of 1250-1450 °C, varied from about 3 to 5 μm/hr (TABLE 1). The maximum growth rate was 5.3 μm/hr at 1250 °C. The enhanced growth rate at this temperature could be a result of higher growth rates of crystal faces that are not (0001) (the growth rate of the smoother area was smaller and comparable to growth at 1300 °C). Error could also be introduced when measuring the growth rate since the top surface is not flat. As the temperature was increased to 1300 and 1350 °C, the growth rate decreased to around 4.2 μm/hr. The growth rate decreased further at higher temperatures (1400 °C and 1450 °C) probably due to precursor depletion before reaching the substrates ($B_{12}P_2$ also deposits on the susceptor walls (see Figure 1)). The films also became thinner along the direction of gas flow due to precursor depletion as the gas passed over the substrate.

3.3. The Epitaxial Relationship as Determined by X-ray Diffraction

The out-of-plane crystallographic relationship between the $B_{12}P_2$ films and the 4H-SiC substrate were determined from XRD scans (FIGURE 4). Three main peaks were observed: (0003) $B_{12}P_2$ at ≈22.5°, (0004) 4H-SiC at ≈35.7°, and (0006) $B_{12}P_2$ at ≈45.9°, confirming that the preferred out-of-plane epitaxial relationship was $(0001)_{B_{12}P_2} \| (0001)_{4H\text{-}SiC}$. A shoulder appeared on the right side of the (0004) 4H-SiC peak after deposition that was not associated with a $B_{12}P_2$ plane. The shoulder is likely a result of strain and distortions in the SiC lattice near the $B_{12}P_2$ interface. $B_{12}P_2$ is a hard material and the epilayers were tensile strained caused by both the lattice constant mismatch and the coefficient of thermal expansion mismatch[23]. The strain is so large that the $B_{12}P_2$ films frequently cracked if they were about 2 μm thick or thicker. Cracks have even been found in the underlying SiC substrate. Domains of cracked areas may cause some peak splitting or broadening. Secondary phases as a result of process gases reacting with the SiC could also potentially play a role.

At the upper and lower temperature bounds (1250 and 1450 °C, respectively), several extra peaks are clearly present, indicating that the films are partially polycrystalline, consistent with the morphological observations. Since both of these films have a $(02\bar{2}4)$ doublet peak located next to the (0006) peak, the $(01\bar{1}2)$ peak may also be present though it is not obvious because the d-spacings

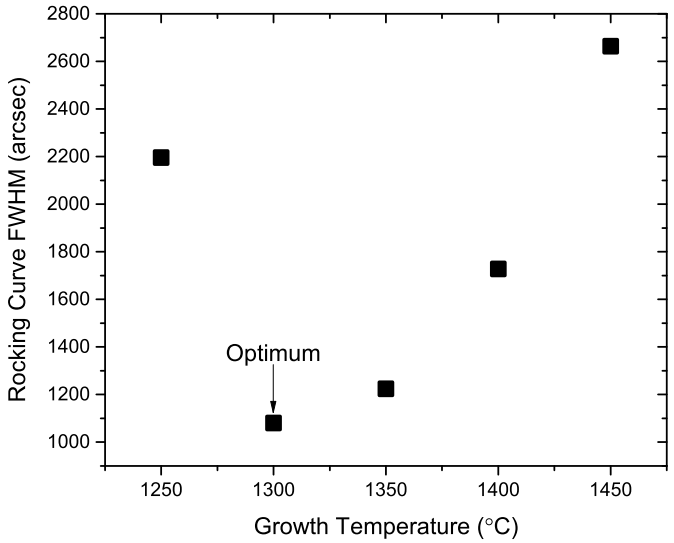

Figure 5: Plot of the X-ray rocking curve FWHM's of $B_{12}P_2$ films grown for 30 min in the temperature range of 1250-1450 °C. The optimum growth temperature is 1300 °C.

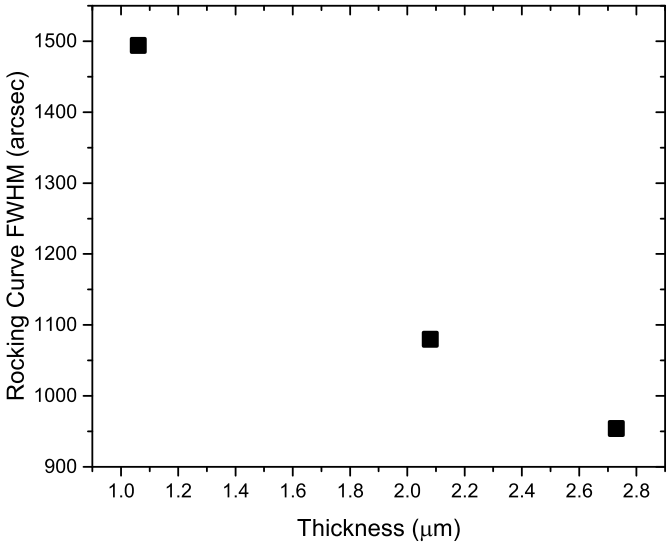

Figure 6: Plot of the X-ray rocking curve FWHM's of $B_{12}P_2$ films grown at 1300 °C for various thicknesses. The crystal quality of the film improves as the thickness increasing, likely due to defect annihilation during continued growth.

of the (0003) and $(01\bar{1}2)$ planes are similar (3.95 and 3.91 Å, respectively), and the peaks overlap. The origin of the $(01\bar{1}2)$ orientation could possibly be a result of strain causing a $(0001)\|(01\bar{1}2)$ twin plane to form[24].

The samples grown from 1300-1400 °C generally have cleaner spectra. The films grown at 1350 and 1400 °C may have a $(02\bar{2}1)$ peak to the left of the (0004) 4H-SiC peak or a shoulder on the (0006) peak caused by a weak adjacent $(02\bar{2}4)$ peak, but the (0001) orientation still dominates. At 1300 °C, the film is a single texture. It also has both the sharpest (0003) and (0006) peaks and the most intense (0003) peak relative to the (0004) 4H-SiC peak, suggesting that films grown at this temperature are higher quality than the others.

To confirm that the $B_{12}P_2$ films are epitaxial to the 4H-SiC, transmission Laue photographs normal to the (0001) plane were taken (not shown) and revealed that the epitaxial relationship between $B_{12}P_2$ and 4H-SiC is $(0001)\langle 11\bar{2}0\rangle_{B_{12}P_2}\|(0001)\langle 11\bar{2}0\rangle_{4H\text{-}SiC}$. This is the same orientation as $B_{12}As_2$ on 4H-SiC[19].

3.4. Effect of Growth Temperature and Film Thickness On XRD Rocking Curve FWHM

While the surface morphology and XRD spectra hint that growth at 1300 °C may produce the highest crystal quality, X-ray rocking curves were taken to quantitatively evaluate the optimum growth temperature. FIGURE 5 depicts the full width at half maximum (FWHM) of the rocking curves of the (0003) $B_{12}P_2$ peak as a function of the growth temperature. At 1250 °C, the film has a FWHM of ≈2200 arcsec which drops sharply to 1080 arcsec at 1300 °C. The polycrystalline overgrowth is likely responsible for the increased FWHM value in the film grown at 1250 °C. The FWHM value increases monotonically above 1300 °C, reaching nearly 2700 arcsec at 1450 °C. Since the minimum value was achieved at 1300 °C, this was the optimum growth temperature for the growth conditions we tested.

The influence of the film thickness on the film quality of $B_{12}P_2$ grown at 1300 °C was also evaluated by measuring the X-ray rocking curve about the (0003) $B_{12}P_2$ peak. As seen in FIGURE 6, the FWHM decreased as the film thickness increased. This trend is also seen in other heteroepitaxial material systems such as GaN on sapphire[25, 26] and 3C-SiC on Si[27] and was most likely due to relaxation of the lattice and annihilation of defects as the films grew thicker[28].

To the authors' knowledge, no rocking curve data has been reported in the literature for $B_{12}P_2$ prior to this publication. While the intrinsic (theoretical minimum) FWHM is unique to every material, a comparison to $B_{12}As_2$ may be the most appropriate since its crystal structure is a direct analog to $B_{12}P_2$. Both Zhang[29] and Nagarajan, *et al.*[30] have reported rocking curve values of the (0003) $B_{12}As_2$ peak on films grown on SiC. Zhang measured FWHM values ranging from 730-812 arcsec over the temperature range of 1200-1350 °C while Nagarajan, *et al.* reported values of 758-1223 arcsec in the range of 1300-1450 °C. The lower FWHM values for $B_{12}As_2$ may be due to fewer dislocations in those films as a result of the smaller lattice mismatch between $B_{12}As_2$ and SiC (∼0.1%) versus that of $B_{12}P_2$ and SiC (∼2.5%).

3.5. Influence of Growth Temperature on Nucleation and Growth Mode

Since the films were grown on vicinal surfaces, ideally the $B_{12}P_2$ should nucleate at a step edge and continue to grow in a step-flow growth mode. However, differences in

surface energy due to the dissimilarity of the epitaxial and substrate materials may drive the growth into an island-type growth regime. The formation of islands elongated in the same direction as the vicinal step edges for growth at 1400 °C (see FIGURE 3b)) suggests that the film nucleated on step edges but then grew in a 3D island growth mode. Further evidence that the films are nucleating on vicinal steps is supported by the suppression of rotational twinning on films grown at 1300 °C on 4H-SiC substrates specifically miscut towards the $(1\bar{1}00)$, which will be reported in a follow up publication.

Above 1350 °C, the films are thought to nucleate as islands which subsequently coalesce into a continuous film. The strong island-type growth caused increased mosaicity in the films and therefore wider rocking curves at the high growth temperatures. Island growth may have been further promoted by an increase in the adatom mobility at higher temperatures. Large adatom diffusion lengths may allow surface atoms to preferentially diffuse to and locate on lower surface energy $B_{12}P_2$ islands over the higher surface energy $B_{12}P_2$/4H-SiC interface, thus minimizing strain in the film.

At 1300 °C or lower, the films were continuous after 15 min of growth (FIGURE 3 a)). At 1250 °C, the films are smooth and continuous down to growth times of 90 seconds. The decreased diffusions lengths at lower growth temperatures may have promoted a 2D growth mechanism by forcing adatoms to attach locally near step edges. Ideally, the diffusion length would be matched to the terrace width of the stepped substrate. While the surface of films grown at 1250 °C for short depositions times were smooth, at longer growth times, i.e. >15 min, the films were dominated by rough polycrystalline growth as seen in FIGURE 2 which prevented growth of quality $B_{12}P_2$ films. This change in growth mode may be attributed to limited adatom diffusion lengths at this low growth temperature, and changes in the precursor flow rates may influence or reduce the formation of the polycrystalline overlayer.

4. Conclusions and Future Work

$B_{12}P_2$ was successfully grown on Si-face (0001) 4H-SiC substrates miscut 4° toward the $(1\bar{1}00)$ from 1250-1450 °C. The optimum growth temperature was 1300 °C as evidenced by XRD rocking curves even though the smoothest film was grown at 1350 °C. The epitaxial relationship is $(0001)\langle 11\bar{2}0\rangle_{B_{12}P_2} \| (0001)\langle 11\bar{2}0\rangle_{4H\text{-}SiC}$. The decrease in the rocking curve FWHM as the film thickness increased suggests that defects are annihilating as the films grow thicker.

Hetero-epitaxy of $B_{12}P_2$ on 4H-SiC can be further improved by modifying the growth conditions to more finely control the growth mode, and further work to optimize the surface structure before epitaxy should be pursued. Ideally, since the films are grown on vicinal surfaces, the adatom diffusion length should be adjusted to match the terrace width to ensure a step flow growth mode. This could be done by fine tuning the growth temperature and adjusting the III/V ratio to control the B and P adatom concentrations which can influence the adatom mean free path and the surface energy. As with many other hetero-epitaxial systems, a buffer layer may improve the crystal quality. To help prevent supersaturation or gas phase nucleation, the B_2H_6 flow rate could be reduced. Further work should also include characterization of the effect of the crystal quality and twinning on the electrical properties of $B_{12}P_2$ films grown on 4H-SiC.

More research could also be done to better understand the stoichiometry of $B_{12}P_2$. Some researchers have reported that $B_{12}P_2$ can accommodate substitutional defects of B atoms located on P sites and that the composition can vary according to $B_{12}(P_{2-x}B_x)$ where x is allowed to be $0 \leq x \leq 1$[16]. It may be possible to measure the compositions of the films indirectly using the volume of the unit cell[16] which can be calculated based on measured lattice constants via XRD. The composition could be different nearer to the substrate than near the film surface, and composition measurements as a function of film thickness could also be done in the future.

This work was performed under the auspices of the U.S. Department of Energy by Lawrence Livermore National Laboratory under Contract DE-AC52-07NA27344, LLNL-JRNL-696569. Material growth was supported by the U.S. Department of Energy, Office of Basic Energy Sciences under Award No. DE-SC0005156.

[1] G. A. Slack, T. F. McNelly, E. A. Taft, Melt growth and properties of B_6P crystals, Journal of Physics and Chemistry of Solids 44 (10) (1983) 1009–1013.

[2] M. Carrard, D. Emin, L. Zuppiroli, Defect clustering and self-healing of electron-irradiated boron-rich solids, Physical Review B 51 (17) (1995) 11270.

[3] T. Stoto, L. Zuppiroli, J. Pelissier, Absence of defect clusters in electron irradiated boron carbide, Radiation effects 90 (3-4) (1985) 161–170.

[4] D. Emin, Unusual properties of icosahedral boron-rich solids, Journal of Solid State Chemistry 179 (9) (2006) 2791–2798.

[5] R. A. Burmeister, P. E. Greene, Synthesis and crystal growth of B_6P, Transactions of the Metallurgical Society of AIME 239 (3) (1967) 408–413.

[6] M. Takigawa, M. Hirayama, K. Shohno, Hetero-epitaxial growth of lower boron phosphide on silicon substrate using PH_3-B_2H_6-H_2 system, Japanese Journal of Applied Physics 12 (10) (1973) 1504.

[7] K. Shohno, M. Takigawa, T. Nakada, Epitaxial growth of BP compounds on Si substrates using the B_2H_6-PH_3-H_2 system, Journal of Crystal Growth 24 (1974) 193–196.

[8] P. Groot, J. H. F. Grondel, P. J. Van der Put, Chemical vapour deposition of boron phosphides using bromide reactants, Solid State Ionics 16 (1985) 95–98.

[9] T. L. Aselage, Preparation of boron-rich refractory semiconductors, in: MRS Proceedings, Vol. 97, Cambridge Univ Press, 1987, p. 101.

[10] Y. Kumashiro, H. Yoshizawa, T. Yokoyama, Epitaxial growth of rhombohedral boron phosphide single crystalline films by chemical vapor deposition, Journal of Solid State Chemistry 133 (1) (1997) 104–112.

[11] P. Lu, J. H. Edgar, J. Pomeroy, M. Kuball, H. M. Meyer, T. Aselage, Growth of rhombohedral $B_{12}P_2$ thin films on 6H-SiC (0001) by chemical vapor deposition, in: MRS Proceedings, Vol. 799, Cambridge Univ Press, 2003, pp. Z2–10.

[12] B. Padavala, C. D. Frye, Z. Ding, R. Chen, M. Dudley,

B. Raghothamachar, N. Khan, J. H. Edgar, Preparation, properties, and characterization of boron phosphide films on 4H-and 6H-silicon carbide, Solid State Sciences 47 (2015) 55–60.
[13] G. Li, J. K. Abbott, J. D. Brasfield, P. Liu, A. Dale, G. Duscher, P. D. Rack, C. S. Feigerle, Structure characterization and strain relief analysis in CVD growth of boron phosphide on silicon carbide, Applied Surface Science 327 (2015) 7–12.
[14] B. Padavala, C. D. Frye, X. Wang, B. Raghothamachar, J. H. Edgar, CVD growth and properties of boron phosphide on 3C-SiC, Journal of Crystal Growth 449 (2016) 15–21.
[15] T. Chu, J. Jackson, A. Hyslop, S. Chu, Crystals and epitaxial layers of boron phosphide, Journal of Applied Physics 42 (1) (1971) 420–424.
[16] G. A. Slack, K. E. Morgan, Some crystallography, chemistry, physics, and thermodynamics of $B_{12}O_2$, $B_{12}P_2$, $B_{12}As_2$, and related alpha-boron type crystals, Journal of Physics and Chemistry of Solids 75 (9) (2014) 1054–1074.
[17] Y. Gong, M. Tapajna, S. Bakalova, Y. Zhang, J. H. Edgar, M. Dudley, M. Hopkins, M. Kuball, Demonstration of boron arsenide heterojunctions: A radiation hard wide band gap semiconductor device, Applied Physics Letters 96 (22) (2010) 223506–223506.
[18] Y. Zhang, H. Chen, M. Dudley, Y. Zhang, J. H. Edgar, Y. Gong, S. Bakalova, M. Kuball, L. Zhang, D. Su, et al., Mechanism for improved quality $B_{12}As_2$ epitaxial films on (0001) 4H-SiC substrates by tilting toward $[1\bar{1}00]$ direction, in: MRS Proceedings, Vol. 1246, Cambridge Univ Press, 2010, pp. 1246–B04.
[19] Y. Zhang, H. Chen, M. Dudley, Y. Zhang, J. H. Edgar, Y. Gong, S. Bakalova, M. Kuball, L. Zhang, D. Su, et al., Growth mechanisms and defect structures of $B_{12}As_2$ epilayers grown on 4H-SiC substrates, Journal of Crystal Growth 352 (1) (2012) 3–8.
[20] B. Padavala, Epitaxy of boron phosphide on AlN, 4H-SiC, 3C-SiC and ZrB_2 substrates, Ph.D. thesis.
[21] V. Ramachandran, M. F. Brady, A. R. Smith, R. M. Feenstra, D. W. Greve, Preparation of atomically flat surfaces on silicon carbide using hydrogen etching, Journal of Electronic Materials 27 (4) (1998) 308–312.
[22] F. Owman, C. Hallin, P. Mårtensson, E. Janzen, Removal of polishing-induced damage from 6H-SiC (0001) substrates by hydrogen etching, Journal of Crystal Growth 167 (1) (1996) 391–395.
[23] C. E. Whiteley, M. J. Kirkham, J. H. Edgar, The coefficients of thermal expansion of boron arsenide ($B_{12}As_2$) between 25 °C and 850 °C, Journal of Physics and Chemistry of Solids 74 (5) (2013) 673–676.
[24] Q. An, W. A. Goddard III, Boron suboxide and boron subphosphide crystals: Hard ceramics that shear without brittle failure, Chemistry of Materials 27 (8) (2015) 2855–2860.
[25] L. S. McCarthy, N. Q. Zhang, H. Xing, B. Moran, S. DenBaars, U. K. Mishra, High voltage AlGaN/GaN heterojunction transistors, International Journal of High Speed Electronics and Systems 14 (01) (2004) 225–243.
[26] D. Kapolnek, X. H. Wu, B. Heying, S. Keller, B. P. Keller, U. K. Mishra, S. P. DenBaars, J. S. Speck, Structural evolution in epitaxial metalorganic chemical vapor deposition grown GaN films on sapphire, Applied Physics Letters 67 (11) (1995) 1541–1543.
[27] M. Wilhelm, M. Rieth, M. Brandl, R. A. Wibowo, R. Hock, P. Wellmann, Optimization of growth parameters for growth of high quality heteroepitaxial 3C–SiC films at 1200 °C, Thin Solid Films 577 (2015) 88–93.
[28] H. Chen, G. Wang, M. Dudley, L. Zhang, L. Wu, Y. Zhu, Z. Xu, J. H. Edgar, M. Kuball, Defect structures in $B_{12}As_2$ epitaxial layers grown on (0001) 6H-SiC, Journal of Applied Physics 103 (12) (2008) 123508.
[29] Y. Zhang, Epitaxial growth of icosahedral boron arsenide on silicon carbide substrates: improved process conditions and electrical properties, Ph.D. thesis, Kansas State University (2011).
[30] R. Nagarajan, Z. Xu, J. H. Edgar, F. Baig, J. Chaudhuri, Z. Rek, E. A. Payzant, H. M. Meyer, J. Pomeroy, M. Kuball, Crystal growth of $B_{12}As_2$ on SiC substrate by CVD method, Journal of Crystal Growth 273 (3) (2005) 431–438.

© 2016. This manuscript version is made available under the CC-BY-NC-ND 4.0 license http://creativecommons.org/licenses/by-nc-nd/4.0/